Supporting Information

Formulating an Ideal Protein Photoresist for Fabricating Dynamic Microstructures with High Aspect Ratios and Uniform Responsiveness

Chee Leng Lay,[†,‡] Yih Hong Lee,[†] Mian Rong Lee,[†] In Yee Phang,[*,‡] Xing Yi Ling[*,†]

[†]Division of Chemistry and Biological Chemistry, School of Physical and Mathematical Sciences, Nanyang Technological University, Singapore 637371 Singapore. Email: xyling@ntu.edu.sg

[‡]Institute of Materials Research and Engineering, Agency for Science, Technology and Research (A*STAR), 2 Fusionopolis Way, Innovis, 08-03, Singapore 138634 Singapore. Email: phangiy@imre.a-star.edu.sg

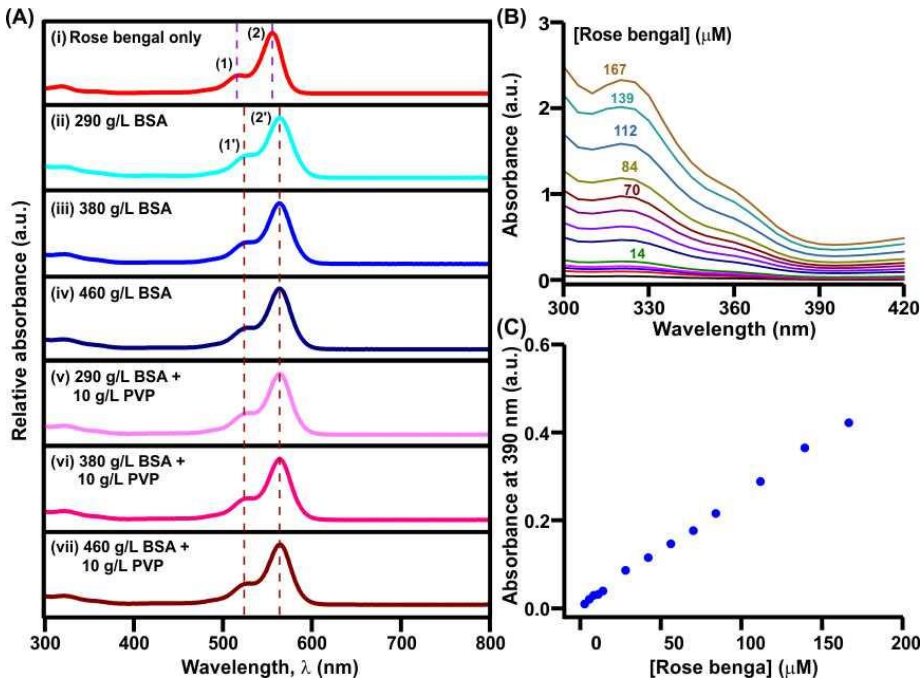

Figure S1. **Effect of BSA and PVP on rose bengal's absorption spectrum.** (**A**) UV-Vis absorption curve of (i) pristine 8.5 mM rose bengal solution and (ii – vii) 8.5 mM rose bengal in different BSA photoresists. 2 μL of sample solutions were diluted in 3 mL of solvent containing 82 v/v % HEPES buffer solution and 18 v/v % DMSO prior to UV-Vis measurements. Relative absorbance is obtained by dividing absorbance at specific wavelength over maximum absorbance. Absorption peaks (peak 1 at λ = 518 nm ; peak 2 at λ = 556 nm) of rose bengal are slightly red-shifted (peak 1' at λ = 527 nm ; peak 2' at λ = 564 nm) when rose bengal molecules are mixed with BSA. The presence of PVP has insignificant effect on rose bengal's absorption. (**B**) Dependence of absorption spectra on rose bengal concentration measured by diluting sample solution containing 8.5 mM rose bengal, 460 g/L BSA and 10 g/L PVP to obtain rose bengal concentration range from 3 μM to 167 μM. (**C**) Graph extracted from (**B**) to illustrate the linear relationship between absorbance at 390 nm as a function of rose bengal concentration, where absorbance = 0.00252 x [RB] with R^2 = 0.9988.

Increasing BSA concentration and addition of PVP do not affect photochemical polymerization and cross-linking processes of the photoresists since the BSA photoresists have similar UV-Vis absorption spectra and laser power threshold, before and after increasing BSA concentration and adding PVP (Figures S1 and S2). Linear concentration

dependence of absorbance on rose bengal concentration at 390 nm is also independent of BSA concentration and presence of PVP (Figures S1B and S1C). Our results are in consistent with findings which reported independence of rose bengal-sensitized photodynamic cross-linking of proteins on addition of acrylamide copolymers[1, 2] or dye-labelled long-chain dextran.[3]

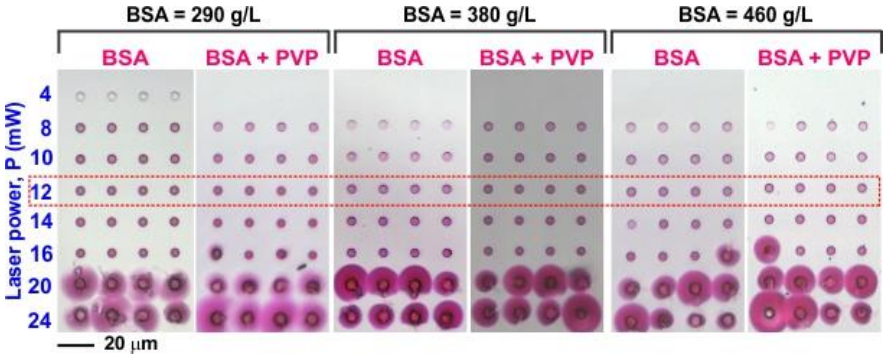

Figure S2. Effect of average laser power, BSA concentration and presence of PVP on photo-polymerizability of BSA photoresists using two-photon lithography. Optical microscopy images of microstructures taken at pH 5. Microstructures are fabricated from different BSA photoresists over laser power ranging from 4 to 24 mW, with constant scan speed of 30 μm/s. Concentration of rose bengal in each BSA photoresist is fixed at 8.5 mM. Swelling capability of microstructures fabricated from different BSA photoresists at 12-mW laser power is compared in Figure 2C.

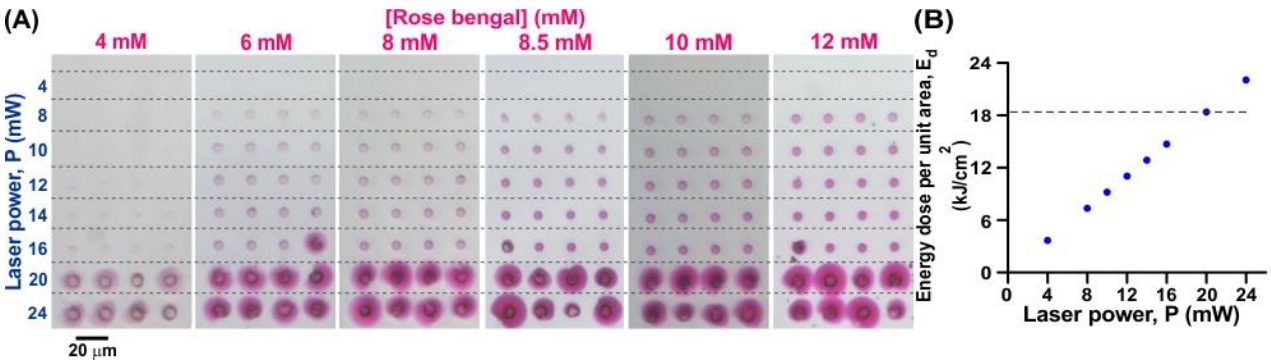

Figure S3. Effect of average laser power and rose bengal concentration on efficiency of two-photon induced polymerization of BSA photoresists. (**A**) Optical microscopy images illustrating influence of laser power and concentration of rose bengal on polymerizability of BSA photoresists when subjected to two-photon lithography. Microstructures are fabricated from BSA solutions containing 460 g/L BSA, rose bengal with concentration of 4 mM to 12 mM, 82 v/v % HEPES buffer solution and 18 v/v % DMSO and are written at laser power ranging from 4 to 24 mW, with constant scan speed of 30 μm/s. Images are taken at their original state in pH 5 solution after development. (**B**) Calculated energy dose per unit area versus applied average laser power. Regions exposed to energy dose per unit area ≥ 18.2 kJ/cm^2 experience internal burning and microstructure explosion (Figures 3 and S3A).

The following equations are used to calculate (i) number of initiating rose bengal molecules within focal volume[4] and (ii) energy dose per unit area.[5] The equations describe the ideal scenario where every dye molecule is efficiently converted to a photochemical reaction trigger after undergoing an absorption event within the laser focal volume.[4] It also assumes that the laser lateral spot size (A) has insignificant change with respect to properties of the photoresist and processing parameters.[5]

(i) <u>Number of initiating rose bengal molecules within focal volume (N_{RB})</u>

P = Laser power (W)

t = Laser dwell time (s)

g_p = 0.664 (Parameter describes pulse shape of Fourier-transform-limited pulse)

τ = Pulse bandwidth = 1×10^{-13} s

f = Laser repetition rate = 8×10^{7} s^{-1}

λ = Excitation wavelength = 7.8×10^{-5} cm

h = Planck's constant = 6.626×10^{-34} J s

c = Speed of light in vacuum = 3×10^{10} cm/s

A = Laser lateral spot size

$= \pi \times [(0.61 \times \lambda)/(\text{Numerical aperture of objective lens})]^2$

$= \pi \times [(0.61 \times 7.8 \times 10^{-5})/ 1.4]^2$

$= 3.629 \times 10^{-9}$ cm^2

N = Number of two-photon absorbing molecules (molecules/cm^3)

ϕ = Quantum efficiency for conversion of excited states to polymerization initiating species

= 1 (rose bengal molecules have quantum efficiency > 98 %)[3, 6]

δ = Two-photon absorption cross-section of rose bengal at the excitation wavelength

$= 10 \times 10^{-50}$ cm^4 s/photon

As a demonstration by using $P = 1.2 \times 10^{-2}$ W, t = 0.0033 s and $N = 5.117 \times 10^{18}$ molecules/cm^3:

$N_{RB} = 0.5 \times [(g_p N \phi \delta) / (\tau f)] \times [\lambda / (h c)]^2 \times (P / A)^2 \times t$

$= 0.5 \text{ x } [(0.664 \times 5.117 \times 10^{18} \times 1 \times 10 \times 10^{-50}) / (1 \times 10^{-13} \times 8 \times 10^{7})] \times [7.8 \times 10^{-5} / (6.626 \times 10^{-34} \times 3 \times 10^{10})]^2 \times (1.2 \times 10^{-2} / 3.629 \times 10^{-9})^2 \times 0.0033$

$= 1.192 \times 10^{22}$ radicals/cm^3

(ii) <u>Energy dose per unit area (E_d)</u>

As a demonstration by using $P = 1.2 \times 10^{-2}$ W and $t = 0.0033$ s,

$E_d = (P \times t) / A$

$= (1.2 \times 10^{-2} \times 0.0033) / 3.629 \times 10^{-9} / 1000$

$= 11.0$ kJ/cm^2

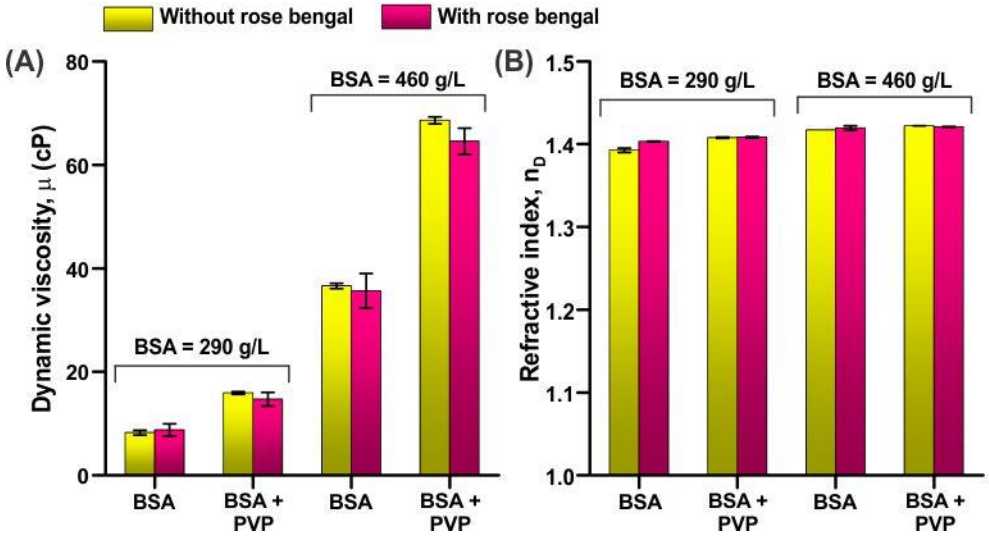

Figure S4. **Effect of rose bengal on the dynamic viscosity and refractive index of BSA photoresists.** (**A**) Dynamic viscosity and (**B**) refractive index of BSA sample solutions with or without rose bengal. Addition of rose bengal has little interference on physical properties of BSA sample solutions.

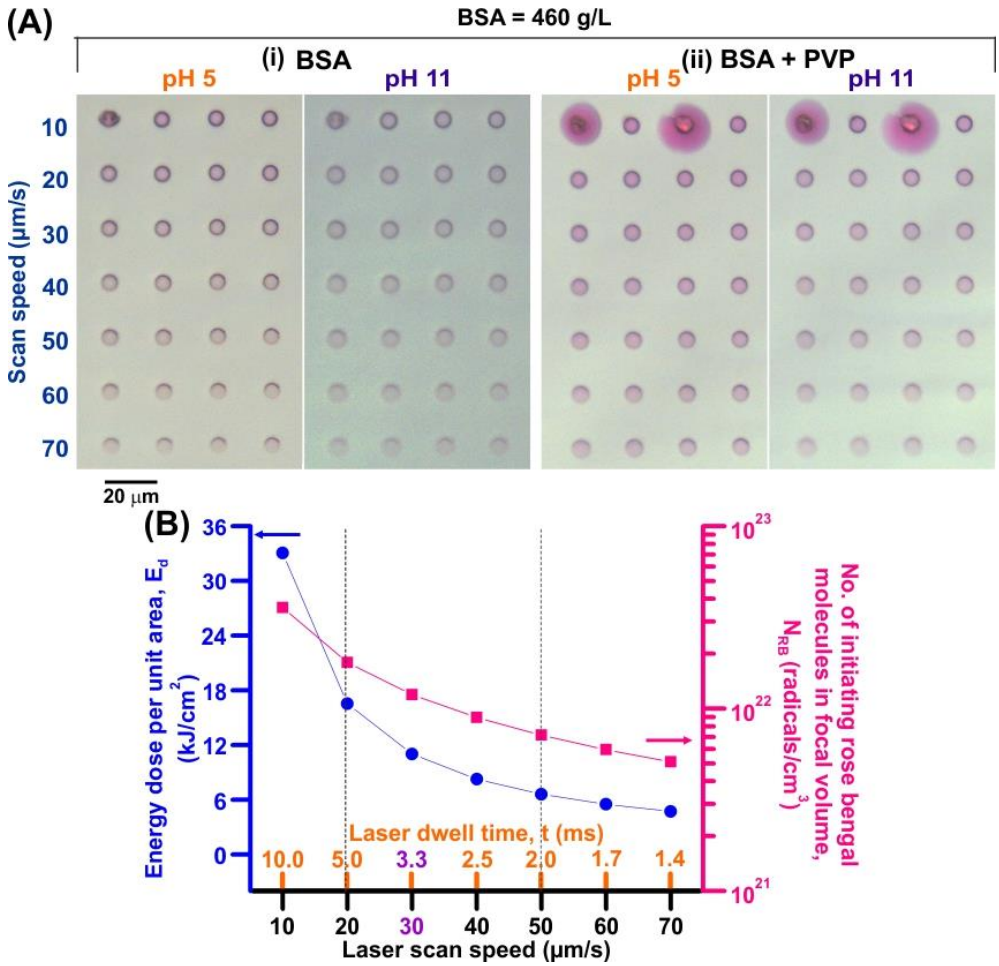

Figure S5. Influence of laser scan speed on fabrication of BSA microstructures. (**A**) Optical microscopy images of microstructures fabricated over laser scan speeds ranging from 10 to 70 mW at constant average laser power of 12 mW. BSA photoresists containing 460 g/L BSA and 8.5 mM rose bengal, (i) without PVP and (ii) with addition of 10 g/L PVP. Images are taken at their original state in pH 5 solution after development. (**B**) Graph illustrates the dependence of calculated energy dose per unit area and number of initiating rose bengal molecules in focal volume on laser dwell time. Theoretical data assume rose bengal molecules within the focal volume are all excited upon irradiation. Well-defined microstructures can be fabricated between laser dwell time of 2.0 ms and 5.0 ms.

Laser scan speed is defined as the speed of focused laser beam travels between irradiated spots, which is inversely proportional to laser dwell time. Laser dwell time is calculated by dividing point distance (distance between laser irradiated spots) over laser scan speed.[5] For consistency, point distance is fixed at 100 nm in all experiments.

To understand the effect of laser scan speed on two-photon induced polymerization of BSA photoresists containing 460 g/L BSA and 460 g/L BSA with 10 g/L PVP, circular microstructures are fabricated from both BSA photoresists over laser scan speed ranged from 10 μm/s to 70 μm/s (Figures 3D and S5A). At very low laser scan speed such as 10 μm/s, microstructures are burnt due to prolonged laser exposure induced accumulation of thermal energy within the confined volume interacts with focused laser beam (laser dwell time = 10 ms; energy dose per unit area = 33.0 kJ/cm^2) (Figure S5). On the other hand, fast laser scan speed minimizes interaction between laser beam and BSA photoresist, and hence less rose bengal molecules are photo-initiated for subsequent photochemical polymerization and cross-linking reactions. As such, microstructures fabricated at too high laser scan speed are not well-constructed. Using equations mentioned in Figure S3, we obtain data points for plotting Figure S5B.

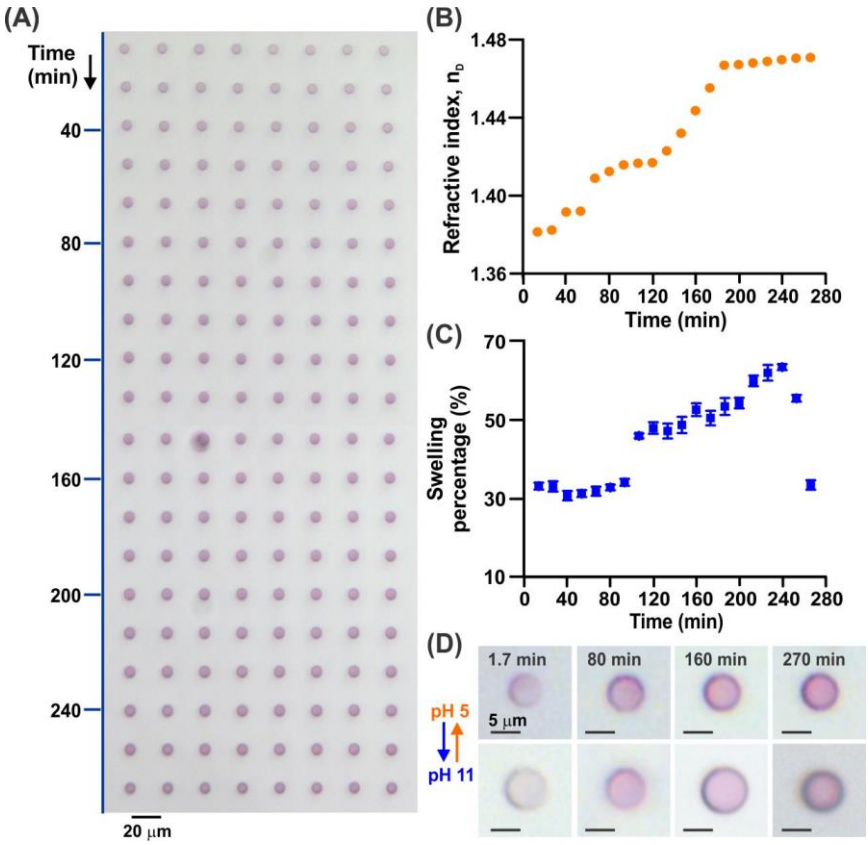

Figure S6. **Photoresist properties and responsiveness of BSA microstructures against fabricating time.** (**A**) Optical microscopy images of an array of BSA microstructures fabricated over 4.4 hours. (**B**) Refractive index (n_D) of sample solutions determined at time of writing completion for each row of eight microstructures. Average standard deviation of refractive index is 0.0040. (**C**) Swelling percentage of fabricated microstructures when immersed in pH 11 solution. Swelling percentage is calculated by dividing the area difference observed between pH 11 and pH 5 over the original area measured at pH 5. (**D**) Optical microscopy images of selected circular microstructures fabricated at different times. BSA circular microstructures are fabricated from BSA photoresist containing 290 g/L BSA and 8.5 mM of rose bengal with laser power of 12 mW at 30 μm/s scan speed.

It is observed that BSA photoresist containing 290 g/L BSA needs approximately two-hour of evaporation before obtaining microstructures with considerable percentage of swelling and structural integrity (Figure S6). Microstructures constructed from BSA photoresist containing 290 g/L BSA with as-discussed processing parameters (laser power =

12 mW, laser scan speed = 30 μm/s) display significant difference in location- and time-dependent physical appearance and swelling behaviours over the 4.4 hours. Since the BSA photoresist has too low BSA monomers to be polymerized and cross-linked within the volume of focused laser beam during microfabrication, leading to microstructures fabricated at initial stage with poor integrity (Figure S6D, 1.7 min to 80 min). As water content is purposely left decreasing over time via evaporation, there is gradual increment in both concentration of BSA and rose bengal from 0 min to 120 min, as reflected from refractive index of the BSA photoresist (refractive index of BSA photoresist changes from 1.3814 at 0 min to 1.4170 at 120 min). As shown in Figure S6B, refractive index of BSA photoresists increases with increasing BSA concentration. The swelling percentage of BSA microstructures also raises from (31 ± 2)% to (48 ± 2)%. It is an indication that more BSA molecules are polymerized and cross-linked within the laser focal volume. After the swelling percentage reaches its maximum at 70 % when BSA photoresist is almost dried out at 240 min, the swelling percentage drops to 34 % at the end of fabrication. The BSA photoresist becomes highly concentrated with BSA, rose bengal and salt when drying, causing the photoresist turn into a solid film around 240 min. Although microstructures fabricated after 240 min have good structural integrity, their response to pH stimulus regress to the swelling percentage of microstructures with poor integrity fabricated between 0 min and 80 min (Figure S6C). This phenomenon is opposed to results obtained from BSA photoresists containing 460 g/L BSA and PVP-incorporated counterparts which are two-photon lithography processable without extra evaporation step (Figure 4).

Besides manually measuring dynamic viscosity and refractive index of the BSA photoresist at different time interval, a sub-system of Nanoscribe called “Definite Focus” from Carl Zeiss automatically detects the change in refractive index between glass substrate and BSA photoresist at a specific position and generate a value termed “interfacial strength”

before the focused laser beam starts writing a new circular microstructure at a specific position. Interfacial strengths measured at 160 locations throughout the fabrication constantly change with fabrication time. The displayed interfacial strength at time 0 s of first position has an initial value of 1766 @ 50 and a final value of 429 @ 1 at the 160th position before the last microstructure was written. On the other hand, for photoresist containing 460 g/L BSA and 10 g/L PVP, no significant deviation is observed for interfacial strengths measured at 160 locations throughout the fabrication. The displayed interfacial strength at time 0 s of first position is 1423 @ 33 and 1593 @ 29 at the 160th position before the last microstructure is written (Figure 4).

These promising results emphasize the feasibility of monitoring dynamic viscosity and refractive index of the liquid photoresists for reproducibility evaluation if fabricated microstructures or patterns have consistent material properties and uniform responsiveness.

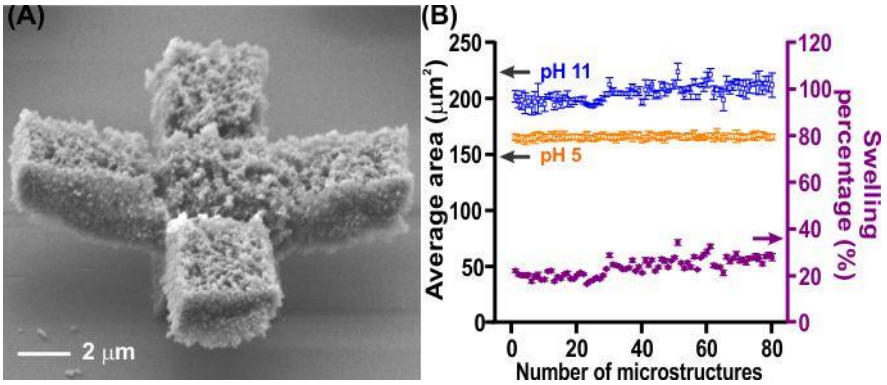

Figure S7. Free-standing microstructures with reproducible consistent responsiveness and structural integrity. (**A**) SEM micrograph (50° tilted view) of an enlarged representative BSA cross-shaped microstructure among 80 free-standing cross-shaped BSA microstructures obtained after de-swelling in pH 5 solution and freeze-drying (Figure 4). (**B**) Average area and swelling property of individual free-standing cross-shaped microstructures of the array. BSA photoresist contains 460 g/L BSA, 10 g/L PVP and 8.5 mM rose bengal. Microstructures are written with laser power of 12 mW at 30 μm/s scan speed.

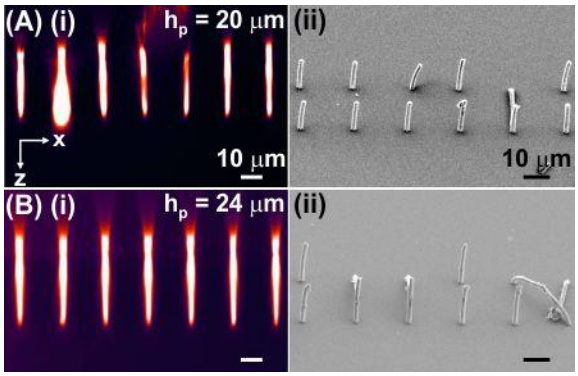

Figure S8. Mechanically unstable micropillars. BSA micropillars fabricated from photoresist containing 460 g/L BSA and 10 g/L PVP with aspect ratio of (**A**) 14.2 (height (h_p) = 20 μm) and (**B**) 17.0 (height (h_p) = 24 μm). (i) Full-width half-maximum (fwhm) intensity profiles of x-z Raman images at pH 5 and (ii) SEM micrographs of the micropillars (40° tilted view).

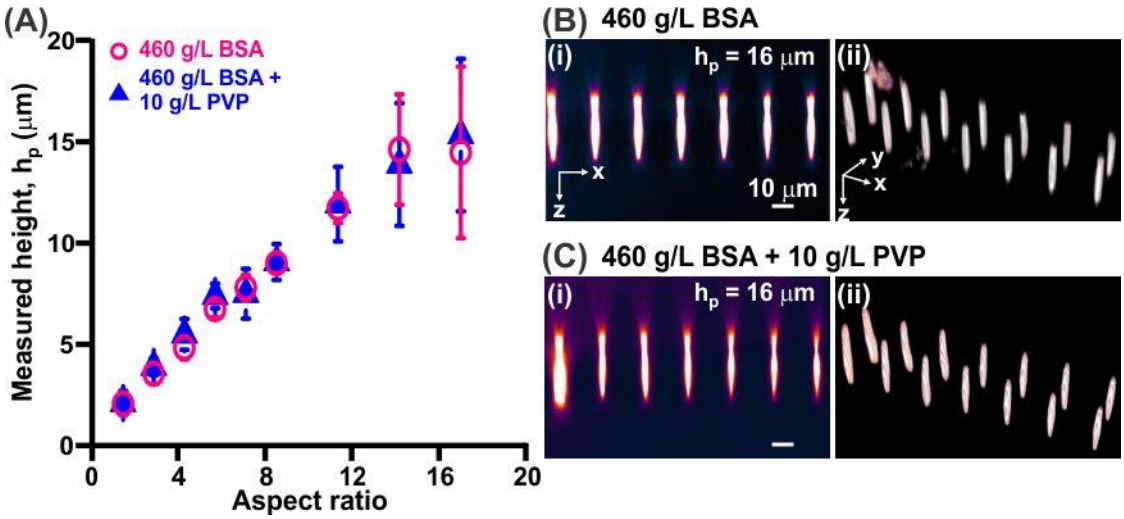

Figure S9. Fabrication of high aspect ratio micropillars. (**A**) Actual height of micropillars of various aspect ratios is determined via measuring the full-width half-maximum (fwhm) intensity profiles of their x-z Raman images at pH 5 (Figure S9Bi-Ci). (**B-C**) (i) Two-dimensional (x-z) and (ii) three-dimensional Raman images of an array of micropillars (height (h_p) = 16 μm; aspect ratio = 11.3) made of BSA sample solutions containing (**B**) 460 g/L BSA and (**C**) 460 g/L BSA with 10 g/L PVP to illustrate integrity of the micropillars in pH 5 solution.

To explore the feasibility of fabricating high aspect ratio protein micropillars using two-photon lithography, we fabricate micropillars with aspect ratio up to 11.3 from BSA photoresists containing either 460 g/L BSA or 460 g/L BSA and 10 g/L PVP. The measured actual heights of these micropillars fabricated from both of the photoresists display similar trend where height of micropillars measured in pH 5 solution constantly increases with as-designed aspect ratio and starts tapering off at aspect ratio of 11.3 (h_p = 16 μm) (Figure S9A). The micropillars are not stiff enough to withstand weight of structures as pillar height is further increased to 20 μm and 24 μm (Figure S8).

Deviation in measured fwhm heights and theoretical as-designed height of micropillars might be attributed to vibrational movement of the motorized stage in z-direction

resulting in poor axial sectioning resolution of the Raman imaging along x-z plane in our photoresist. As such, the system might not be sensitive enough to detect minute changes in the height of micropillars. Nevertheless, Raman imaging and fwhm measurements verify high structural integrity of the as-fabricated micropillars which survived from soaking and rinsing in PBS buffered solution for two days during development and Raman imaging.

REFERENCES

(1) Basu, S.; Campagnola, P. J. Enzymatic Activity of Alkaline Phosphatase Inside Protein and Polymer Structures Fabricated via Multiphoton Excitation. *Biomacromolecules* **2004**, *5*, 572-579.

(2) Shen, H.-R.; Spikes, J. D.; Kopečeková, P.; Kopeček, J. Photodynamic cross-linking of proteins. I. Model Studies Using Histidine- and Lysine-Containing N-(2-Hydroxypropyl) Methacrylamide Copolymers. *J. Photochem. Photobiol. B: Biol.* **1996**, *34*, 203-210.

(3) Pitts, J. D.; Campagnola, P. J.; Epling, G. A.; Goodman, S. L. Submicron Multiphoton Free-Form Fabrication of Proteins and Polymers: Studies of Reaction Efficiencies and Applications in Sustained Release. *Macromolecules* **2000**, *33*, 1514-1523.

(4) Leatherdale, C. A.; DeVoe, R. J. In *Two-Photon Microfabrication Using Two-Component Photoinitiation Systems: Effect of Photosensitizer and Acceptor Concentrations*, *Nonlinear Optical Transmission and Multiphoton Processes in Organics*, Bellingham, WA; Yeates, A. T., Belfield, K. D., Kajzar, F., Lawson, C. M., Eds.; SPIE Proceedings: Bellingham, WA, 2003; pp 112-123.

(5) Serien, D.; Takeuchi, S. Fabrication of Submicron Proteinaceous Structures by Direct Laser Writing. *Appl. Phys. Lett.* **2015**, *107*, 013702.

(6) Basu, S.; Campagnola, P. J. Properties of Cross-linked Protein Matrices for Tissue Engineering Applications Synthesized by Multiphoton Excitation. *J. Biomed. Mater. Res. A* **2004**, *71A*, 359-368.